

Article

Quasi-Linear Polarized Modes in Y-Rotated Piezoelectric GaPO₄ Plates

Cinzia Caliendo * and Fabio Lo Castro

Istituto di Acustica e Sensoristica Corbino, IDASC-CNR, Via del Fosso del Cavaliere 100, 00133 Roma, Italy; E-Mail: fabio.locastro@idasc.cnr.it

* Author to whom correspondence should be addressed; E-Mail: cinzia.caliendo@idasc.cnr.it; Tel.: +39-6-4548-8741; Fax: +39-6-4548-8061.

Received: 30 April 2014; in revised form: 14 June 2014 / Accepted: 16 June 2014 /

Published: 7 July 2014

Abstract: The propagation of both surface and flexural acoustic plate modes along *y*-rotated *x*-propagation GaPO₄ piezoelectric substrates was studied for several *y*-cut angles: the phase velocity and coupling coefficient dispersion curves were theoretically calculated for two different electroacoustic coupling configurations. The investigation of the acoustic field profile across the plate thickness revealed the presence of thin plate modes having polarization predominantly oriented along the propagation direction, and hence suitable for operation in liquid environment. These modes include the linearly polarized Anisimkin Jr. and the quasi longitudinal plate modes, AMs and QLs, showing a phase velocity close to that of the longitudinal bulk acoustic wave propagating in the same direction. The temperature coefficient of delay (TCD) of these longitudinal modes was investigated in the −20 to 420 °C temperature range, in order to identify thermally stable or low TCD cuts. The power flow angle, *i.e.*, the angle between the phase and group velocity vectors, was also estimated to evaluate the substrate anisotropy effect on the acoustic wave propagation. The GaPO₄ intrinsic properties, such as its resistance to high temperature and its chemical inertness, make it especially attractive for the development of acoustic waves-based sensors for applications in harsh liquid environment.

Keywords: GaPO₄; Anisimkin Jr. modes; quasi longitudinal modes; piezoelectricity

1. Introduction

The electroacoustic devices based on the surface and bulk acoustic waves (SAW and BAW) propagation, such as resonators or delay lines, are known for their wide range of applications in chemical, biological and physical sensing fields. When these devices are required to operate in a liquid environment, they must involve the propagation of specific types of acoustic waves that do not radiate energy into the liquid. The types of acoustic waves that are suitable as the sensing elements in liquid environments include Love waves and surface transverse waves (STW), travelling along the surface of a semi-infinite piezoelectric medium, and shear horizontal acoustic plate modes (SHAPM), travelling along a piezoelectric finite thickness plate. The shear horizontal polarization of these modes ensures no coupling between the liquid and the elastic propagating medium [1]. Waves with elliptical polarization, such as the Rayleigh-like waves, are impractical for use in liquid environments as a consequence of the high energy loss into the liquid. The fundamental antisymmetric Lamb mode, A_0 , while being elliptically polarized, can travel along thin plates that are in contact with a liquid, but only at a specific plate thickness. As a consequence of the A_0 mode dispersive phase velocity, it can be designed to travel at a velocity lower than the compressional velocity of the surrounding liquid medium. The plate acts as a waveguide where the ultrasonic wave energy is confined rather than dispersed into the surrounding medium, and only the evanescent wave penetrates the fluid. The fundamental symmetric Lamb mode, S_0 , as well as the higher order symmetrical and antisymmetrical modes have comparable longitudinal, shear-horizontal and shear-vertical displacement components, and velocity higher than that of the surrounding liquid medium, and thus they are not suitable for sensing application in liquids except in some special cases. These cases include linearly polarized modes, such as the longitudinally polarized Anisimkin Jr. (AMs) and the quasi longitudinal (QLMs) modes, and the quasi shear horizontal (QSH) modes with negligible particle displacement components perpendicular to the plate surfaces. The polarization of the AMs is predominantly longitudinal and uniform through the plate thickness, being the shear vertical and horizontal particle displacement components negligible. A mode is classified as QLM if the longitudinal displacement component is dominant but not constant through the plate thickness, being the other two shear components much smaller than the longitudinal one. The AMs and QLMs, while having high phase velocity (close to that of the longitudinal bulk acoustic wave, LBAW, traveling in the same direction) are suitable for high operation frequency $f = v/\lambda$, being λ the acoustic wavelength and v the mode phase velocity. A sensor based on a high-frequency electroacoustic device exhibits superior performances: The higher the frequency the higher the sensor sensitivity and resolution. AMs were first discovered in quartz plates [2] and then in LiNbO_3 $128^\circ y, x + 90^\circ$ and Te [3]. In reference [4,5] the AM's propagation is studied along many piezoelectric substrates, such as Quartz, LiNbO_3 , LiTaO_3 , Te, $\text{Ba}_2\text{NaNb}_5\text{O}_{15}$, KH_2PO_4 , $\text{Li}_2\text{B}_4\text{O}_7$, TeO_2 , PbMoO_4 , KDP and ZnO. Viscosity sensors with high-sensitivity, low-insertion loss, and good stop-band rejection were implemented on quartz, LiNbO_3 and LiTaO_3 [6]. Unfortunately, the *conventional* piezoelectric materials such as quartz, AlPO_4 , LiNbO_3 and LiTaO_3 , are not suitable to work at high temperature as they undergo α to β phase transition at temperature in the range from about 300 to 588 °C. Unlike these conventional piezoelectric materials, GaPO_4 exhibits stable properties up to 900 °C. It exhibits a high piezoelectric sensitivity and strong electromechanical coupling up to about 970 °C and is fully stable against organic solvents, such as ethanol, isopropanol,

acetone, ethyl-methyl ketone, and dimethylformamide. GaPO_4 is also stable in aqueous solutions in the 3 to 8.5 pH range: outside this range, it is etched, except by concentrated H_2SO_4 [7]. Moreover, GaPO_4 shows performances superior to quartz such as thermal stability, piezoelectric coupling and temperature compensated cuts for BAW and SAW applications. All these properties make GaPO_4 a very attractive choice for a wide range of high-temperature, harsh environment applications, such as for the monitoring of process variables, such as viscosity of melts, evaluation of material integrity in harsh environments, e.g., turbine blades, combustion engines and nuclear reactors.

New viable modes, *i.e.*, the longitudinally polarized plate modes, are here theoretically investigated, that are suitable for sensing application in liquids (e.g., for the determination of density, viscosity, conductivity, permittivity, and detection of small mass changes). Such acoustic modes have not yet been fully exploited for sensing applications, thus their study introduces a new element in the landscape of the acoustic waves (AW) sensor field.

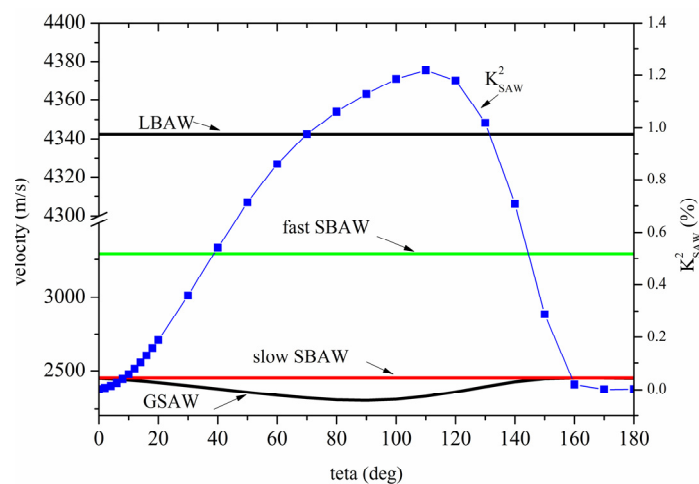
The present paper investigate the acoustic waves propagation along y -rotated x - GaPO_4 substrates for several y -cut angles: The phase velocity, the coupling coefficient, the temperature coefficient of delay (TCD), the power flow angle (PFA) and the acoustic field profile of the propagating modes were investigated that are suitable for application in liquid ambient.

2. Acoustic Wave Propagation in Y-Rotated GaPO_4

2.1. The SAW Propagation in GaPO_4

The SAW propagating along the x direction of a semi-infinite y -rotated GaPO_4 substrate is a generalized SAW (GSAW) as it has three particle displacement components (the longitudinal U_1 , the shear horizontal and vertical, U_2 and U_3) that rapidly decrease in depth. The GSAW phase velocity is strongly affected by the cut angle, as shown in Figure 1 where the angular dispersion velocity curves of the SAW and BAW (the longitudinal BAW, LBAW, and the two transverse BAW, the fast shear, FSBAW, and the slow shear, SSBAW, having velocity equal to 4342.35, 3289.78 and 2451.96 m/s, respectively) are reported.

Figure 1. The bulk acoustic wave (BAW) and generalized surface acoustic wave (GSAW) angular dispersion curves, and the GSAW K_{SAW}^2 angular dispersion curves along ($0^\circ \theta 0^\circ$) GaPO_4 substrate.

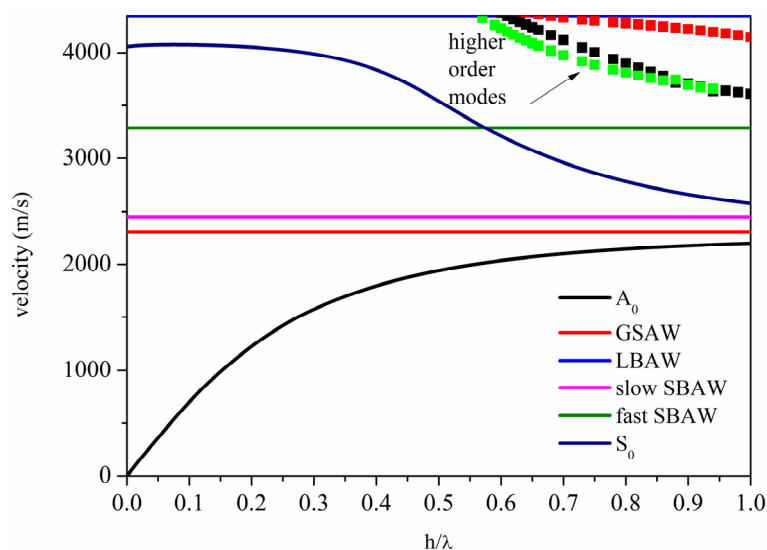


In Figure 1, the angle θ means the amount of rotation around the crystal x axes of a y -cut GaPO_4 plate and is expressed in the Euler notation. The GSAW phase velocity along $(0^\circ \theta 0^\circ)$ GaPO_4 is lower than that of the SBAW except for the $162^\circ \leq \theta \leq 169^\circ$ range. While varying the cut angle and the velocity moving toward the SBAW velocity, the shear horizontal amplitude U_2 of the GSAW decreases more and more slowly in the depth and the GSAW loses energy into the bulk. The electromechanical coupling coefficient, K^2 , is a measure of the electrical to acoustic energy conversion efficiency and it was calculated as $2 \times (v_f - v_m)/v_f$, being v_f and v_m the GSAW velocity along the free surface and the surface covered by a infinitesimally thin conductive film. The K^2 angular dispersion curve is also shown in Figure 1. The highest K^2 value is equal to 1.22% and it is reached at $\theta = 110^\circ$; while the velocity moving toward the SBAW velocity, the GSAW K^2 approaches the zero value, in accordance with the increased U_2 contribution in the depth. The acoustic waves velocity calculations along GaPO_4 were performed by using Matlab and the software from McGill University [8] in the lossless approximation; the GaPO_4 material data (the mass density, the elastic, piezoelectric, dielectric constants) as well as the thermal expansion coefficients and the third order temperature coefficients of the elastic constants, valid in the $-50^\circ\text{C} < T < 700^\circ\text{C}$ temperature range, are referred to [7,9,10], and are those provided by Piezocryst Advanced Sensorics GmbH, which is an European GaPO_4 wafers suppliers.

2.2. The Flexural Plate Waves (FPWs) Propagation in GaPO_4

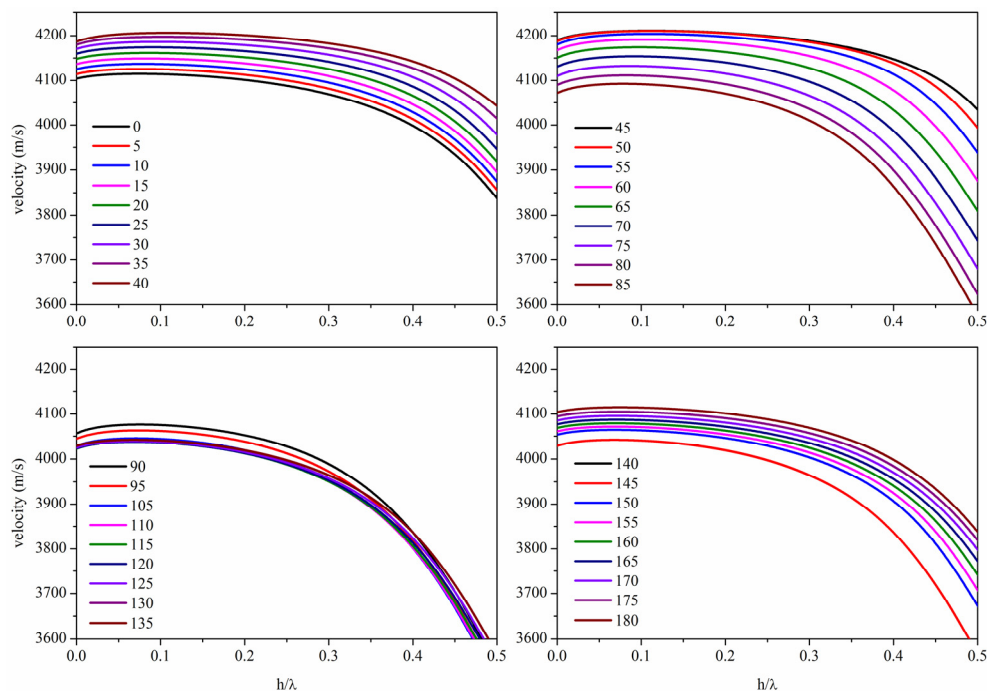
The FPWs propagating along a thin plate consist in two sets of infinite modes: the symmetric waves, whose particle displacements are symmetric about the central plane of the plate, and the antisymmetric waves, whose displacements have odd symmetry about the central plane of the plate. For sufficiently thin plate, only the first symmetric and antisymmetric modes, S_0 and A_0 , propagate: Figure 2 shows the dispersion curves of a few modes propagating along $(0^\circ 90^\circ 0^\circ)$ GaPO_4 plate as an example.

Figure 2. Dispersion curves of the fundamental and higher order modes propagating along $(0^\circ 90^\circ 0^\circ)$ GaPO_4 plate.



The A_0 mode is clearly identified by its reducing velocity as the plate thickness approaches zero. On the contrary, the dispersion curve of the S_0 mode is characterized by a low dispersion region, where its velocity is almost constant and $v \approx v_{\text{LBAW}}$, followed by a drop in velocity. The magnitude of the flat zone of the dispersion curve depends on the rotation angle θ , as can be seen in Figure 3 where the S_0 velocity dispersion curves are shown for different rotating angles and for plate thickness normalized to the acoustic wavelength, h/λ , up to 0.5. The low dispersion region reaches its largest amplitude for $\theta = 40^\circ$.

Figure 3. S_0 velocity dispersion curves for different rotating angles.

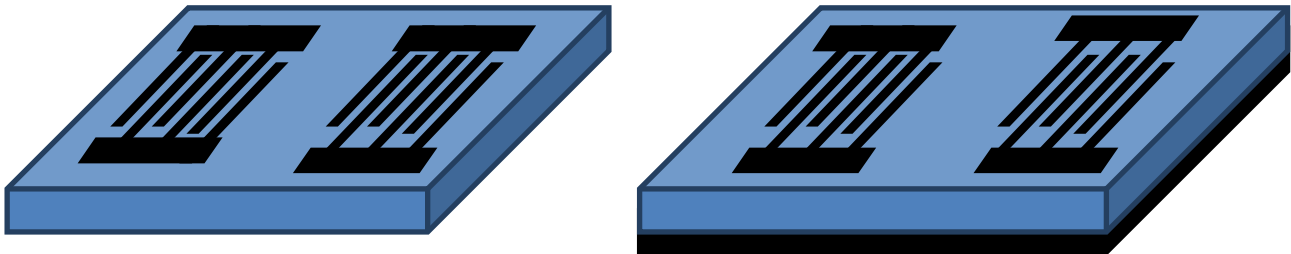


For very small thicknesses, $h/\lambda \ll 0.1$, the S_0 velocity increases slowly and reaches a plateau where the velocity is close to the LBAW velocity. In this flat region, for plate thicknesses up to a value that depends on θ , hereafter mentioned h/λ_{AM} , the S_0 mode transforms for first to the AM counterpart with constant and dominant longitudinal displacement. Subsequently, the mode transforms to the QL counterpart for increasing the plate thicknesses up to h/λ_{QLM} : The longitudinal displacement component is no longer constant through the thickness of the plate and is dominant over the other two components. For higher plate thicknesses, the S_0 mode is characterized by three particle displacement components and, when the velocity approaches the shear horizontal BAW velocity, the U_2 component largely dominates over U_1 and U_3 . For large $h/\lambda > 1$, the mode begins to act as a Rayleigh wave propagating on the surface of the plate: The mode is confined to the surface of the plate to a depth of a few wavelengths and the plate acts as a semi-infinite half space.

In the present paper, the S_0 and A_0 modes propagation along GaPO_4 plates is studied for two different coupling structures as depicted in Figure 4. The configurations called Substrate/Transducer (ST) and Metal/Substrate/Transducer (MST) refer to a plate with one surface that sustain the excitation and detection of the acoustic waves through the interdigital transducers (IDTs), while the opposite surface is free or covered by a ground metal electrode. The FPWs K^2 depends very strongly on θ ,

on the electrical boundary conditions and on the plate thickness. With increasing the plate thickness, for $h/\lambda \gg 1$, the K^2 moves toward the K^2 of the GSAW that propagates along the x direction of the y -rotated cut GaPO₄ semi-infinite substrate.

Figure 4. The Substrate/Transducer (ST) and Metal/Substrate/Transducer (MST) coupling configurations.



The K^2 dispersion curves of the S_0 and A_0 modes were studied for the ST and MST structures by calculating the perturbation of the phase velocity when the tangential electric field component is shorted out at the plate surface. For each configuration K^2 was approximated to be $2 \times [(v_f - v_m)/v_f]$, where v_m and v_f are the phase velocities along the structures with and without the IDTs, under the assumption that a perfect conductor is placed at both the IDT and the ground electrode position. The K^2 dispersion curves of each configuration were calculated for different plate thicknesses normalized to the acoustic wavelength, h/λ , in the range 0.0001 to 2, with 0.0001 h/λ step, in the approximation of infinitesimally-thin perfectly-conductive grounded electrode and IDTs. K^2 values much higher than that of the SAW travelling in the same direction and crystal plane can be reached in thin plates ($h/\lambda \ll 1$), for both S_0 and A_0 modes, even for that cut angles for which the SAW has a $K^2 = 0\%$. The K^2 angular dispersion curves of the S_0 mode in both the ST and MST configurations have similar behavior: The K^2 reaches a peak for small plate thickness (at about $h/\lambda \sim 0.1$ and 0.4 , respectively), then it resets and increases again, and finally it asymptotically reaches the K^2 of the SAW. Figure 5 shows, as an example, the S_0 mode K^2 dispersion curves of the two configurations in $(0^\circ 85^\circ 0^\circ)$ x -GaPO₄. The K^2 dispersion curve of the MST configuration has a second broad peak at $h/\lambda \sim 2$ that is higher than the K^2 of the SAW: With increasing the plate thickness, the K^2 decreases and then, for $h/\lambda \gg 1$, it asymptotically reaches the K^2 of the SAW travelling on the free surface of the plate.

Figure 5. The S_0 mode K^2 dispersion of the two configurations in $(0^\circ 85^\circ 0^\circ)$ x -GaPO₄.

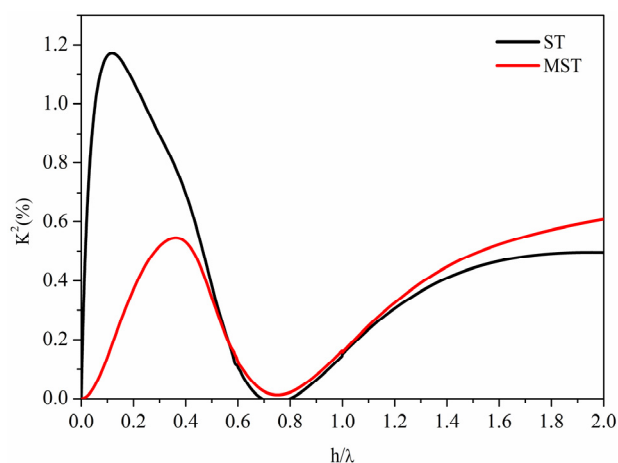
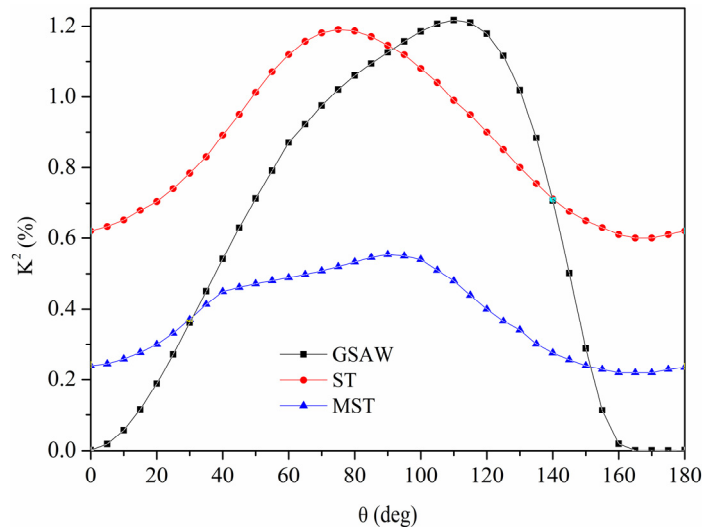


Figure 6 shows the K^2 angular dispersion curve of the SAW travelling along the free plate surface, and the angular dispersion curves of the maximum K^2 value achievable by the S_0 mode for the two coupling configurations. The K^2 peak value of the ST configuration is higher than the K^2 of the SAW for $\theta \leq 90^\circ$ and $>150^\circ$, while that of the MST configuration is higher only for θ ranging from 0° to 30° and $\theta >140^\circ$.

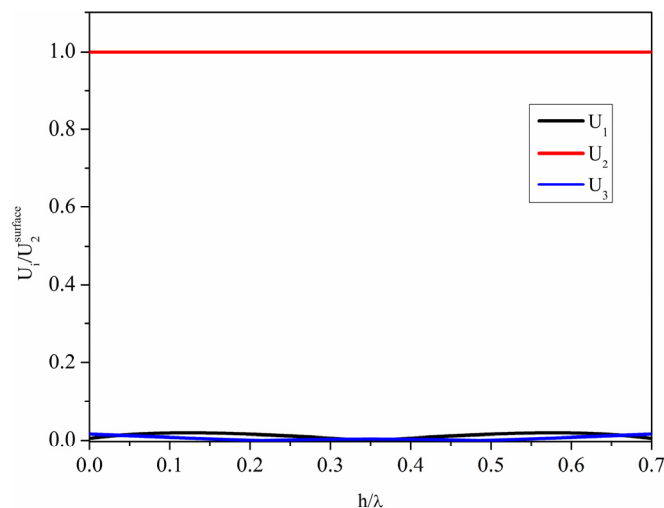
Figure 6. The angular dispersion curves of the maximum K^2 value achievable with the two S_0 mode coupling configurations and the SAW K^2 angular dispersion.



The highest coupling efficiency of the S_0 mode is around 1.2%, and it is reached by the ST configuration at $h/\lambda \sim 0.11$.

As an example, Figure 7 shows the field profile of the shear mode propagating at $v = 3300$ m/s along the $(0^\circ 75^\circ 0^\circ)$ x -GaPO₄ plate with $h/\lambda = 0.11$, for which the conditions $U_2 \gg U_1, U_3$ across the depth are satisfied, and $v \sim v_{SHBAW}$. This type of mode is largely applied for sensing applications in liquid environments [11–13] thanks to its right polarization, but it is disadvantageous compared to the AMs or QLMs as it travels at a lower velocity.

Figure 7. The field profile of the shear horizontal (SH) wave travelling along $(0^\circ 75^\circ 0^\circ)$ x -GaPO₄ plate with $h/\lambda = 0.7$.



The A_0 mode is far more efficient than the S_0 and its most efficient of the two configurations is the MST for all the θ values from 0° to 180° . The K^2 dispersion curves of the A_0 mode depends on θ , on the electrical boundary conditions and on the plate thickness: These curves have a peak value at $h/\lambda \ll 1$, and then asymptotically reach the K^2 of the SAW with increasing the plate thickness. As an example, Figure 8 shows the K^2 dispersion curves of the two A_0 -based configurations on $(0^\circ 95^\circ 0^\circ)$ x -GaPO₄.

Figure 8. The K^2 of the two A_0 coupling configurations on $(0^\circ 95^\circ 0^\circ)$ x -GaPO₄.

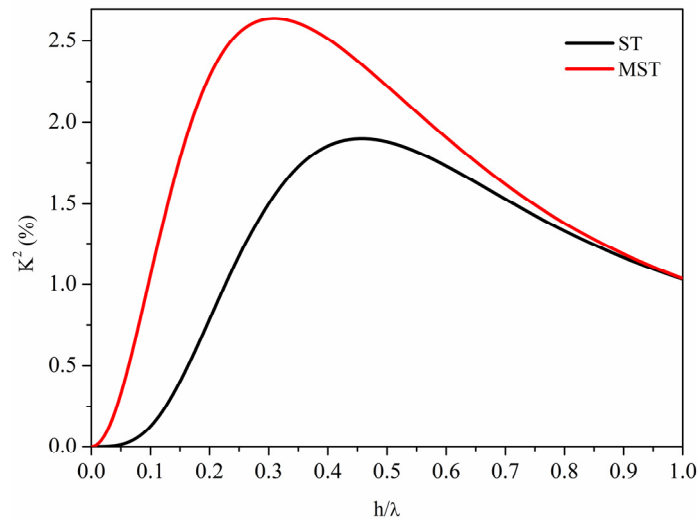
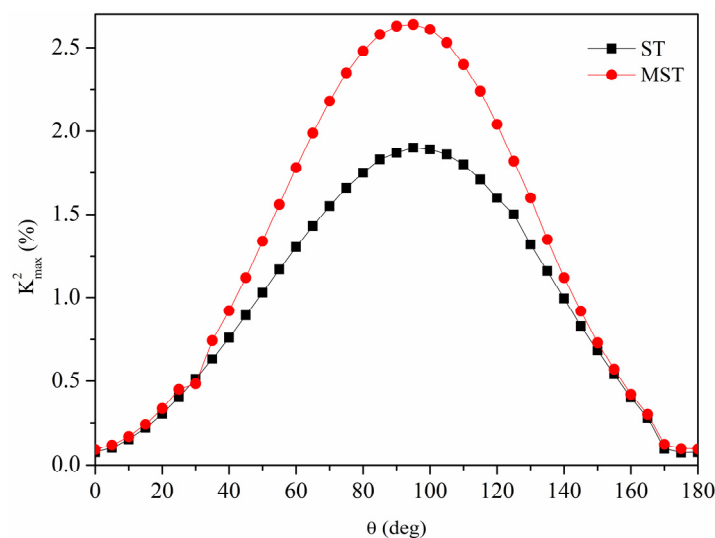


Figure 9 shows the angular dispersion of the K^2 peaks of the A_0 mode for the two coupling configurations. K^2 as high as 1.9% and 2.64% can be reached by the ST and MST configurations for $\theta = 95^\circ$, and for plate thickness equal to $h/\lambda = 0.458$ and 0.31 .

Figure 9. The angular dispersion of the K^2 peaks of the A_0 mode for the two coupling configurations.



The A_0 mode, while being elliptically polarized, can travel along thin membranes that are in contact with a liquid as a consequence of its dispersive phase velocity that can be designed to be lower than the liquid medium compressional velocity, at the proper plate thickness. The phase velocity corresponding

to the K^2 peak values is 1888 and 1583 m/s for the ST and MST configurations, respectively. Thus, a little decrease in K^2 has to be accepted to reduce the velocity of the A_0 mode up to a value lower than the velocity of the fluid environment (about 1500 m/s for water). Another benefit of the low-velocity A_0 mode is that it allows for inexpensive signal processing equipment to be used, due to its low resonant frequency $f = v/\lambda$.

2.3. The Anisimkin Jr. Modes

In references [14,15] the peculiarities of the AMs are so defined: they have a velocity very close to that of the longitudinal BAW and have a dominant longitudinal displacement component U_1 with constant amplitude along the whole depth of the plate, being the shear components, U_2 and U_3 , at least 10 times less than U_1 at any plate depth. The propagation of the AMs was investigated by studying the field profile of the modes that propagate along the plate with a phase velocity close to that of the LBAW: Plate thicknesses up to $h/\lambda = 2$ were studied. As an example, Figure 10 shows the field profile (the three displacement components normalized to the U_1 surface value vs. the plate depth) of the AM propagating along the $(0^\circ 60^\circ 0^\circ)$ x -GaPO₄ plate with $h/\lambda = 0.11$.

Figure 10. The field profile of the Anisimkin Jr. mode (AM) propagating at velocity $v = 4191$ m/s along a $(0^\circ 60^\circ 0^\circ)$ x -GaPO₄ plate $h/\lambda = 0.11$ thick.

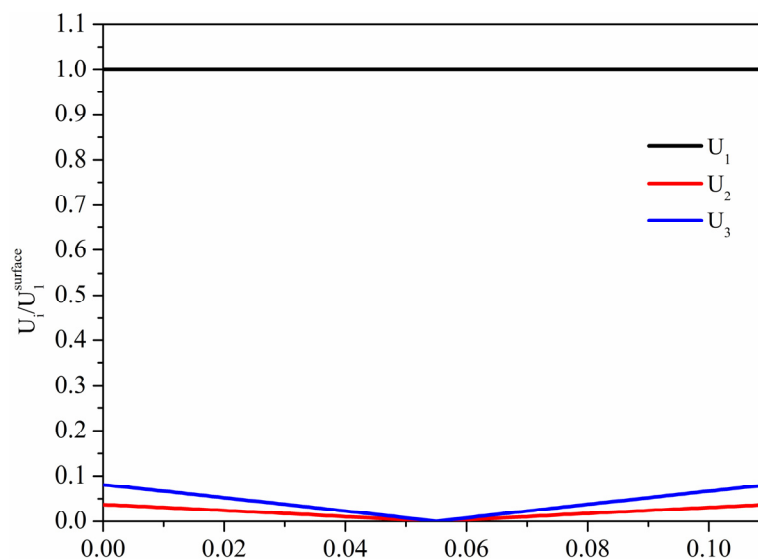
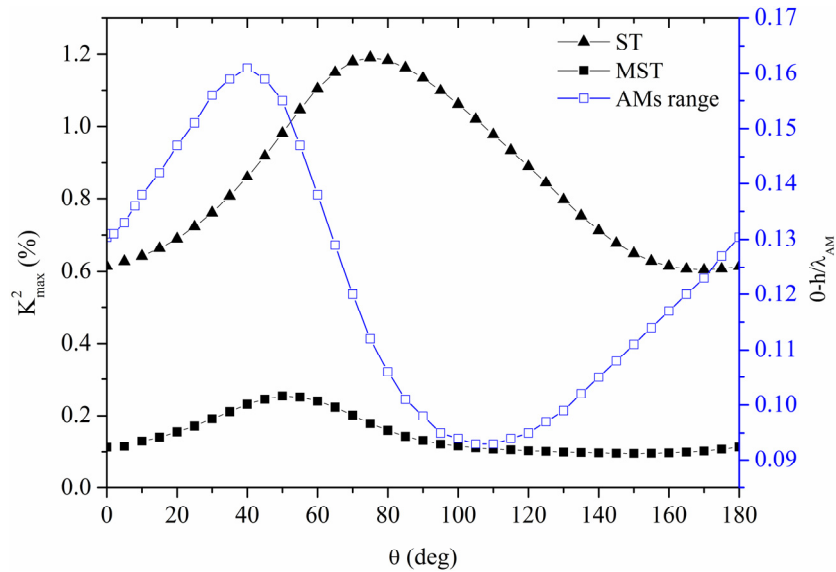


Figure 11 shows the normalized plate thicknesses for which both the conditions $U_1 = 1$, $U_2, U_3 \leq 0.1$ across the plate depth and $v \sim v_{\text{LBAW}}$ are satisfied and the maximum K^2 value achievable in this thickness range, for the ST and MST configurations, as a function of the substrate y -rotation angle. No other plate thickness range suitable for the AMs propagation was found in the 0 to 2 range of h/λ .

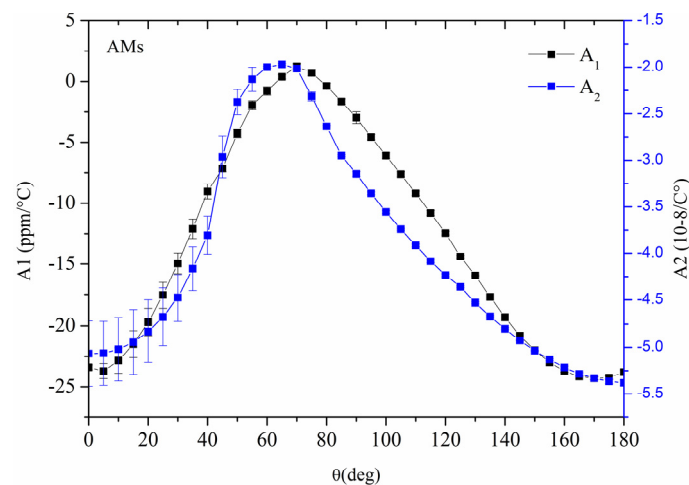
As can be seen, the ST configuration is the most favorable as it ensures the highest K^2 at the largest plate thickness: the latter characteristic is particularly important as it is difficult to fabricate and handle a device implemented on a thin and fragile plate.

Figure 11. The AMs plate thickness range, $0-h/\lambda_{AM}$, and the peak K^2 of the two configurations vs. the rotation angle.



The temperature coefficient of velocity (TCV), $TCV = (1/T^{\circ C})(v_{T^{\circ C}} - v_{20^{\circ C}})/v_{20^{\circ C}}$, that is linked to the TCD by the relation $TCD = \alpha - TCV$, being α the thermal expansion coefficient of the plate, was calculated over the plate thickness range, $0.001-h/\lambda_{AMs}$, over which the AMs propagate. The calculated TCV is referred to $20^{\circ C}$, being $v_{T^{\circ C}}$ and $v_{20^{\circ C}}$ the wave velocity at a certain temperature value between -20 and $420^{\circ C}$, and at $20^{\circ C}$, respectively. The relative velocity shift $(v_{T^{\circ C}} - v_{20^{\circ C}})/v_{20^{\circ C}}$ vs. temperature curves, calculated for different h/λ values in the $0.001-h/\lambda_{AMs}$ range for each y -rotation angle, were then fitted by a quadratic function. Figure 12 shows the first and second order coefficients A_1 and A_2 of the quadratic fit: The bar centered on each point refers to the coefficient evaluated at the upper (h/λ_{AMs}) and lower (0.001) plate thickness range. As can be seen in Figure 12, for $\theta \geq 55^{\circ}$, the two coefficients are poorly affected by the plate thickness change over the $0.001-h/\lambda_{AMs}$.

Figure 12. The first and second order coefficients, A_1 and A_2 , of the temperature coefficient of velocity (TCV) quadratic fit.



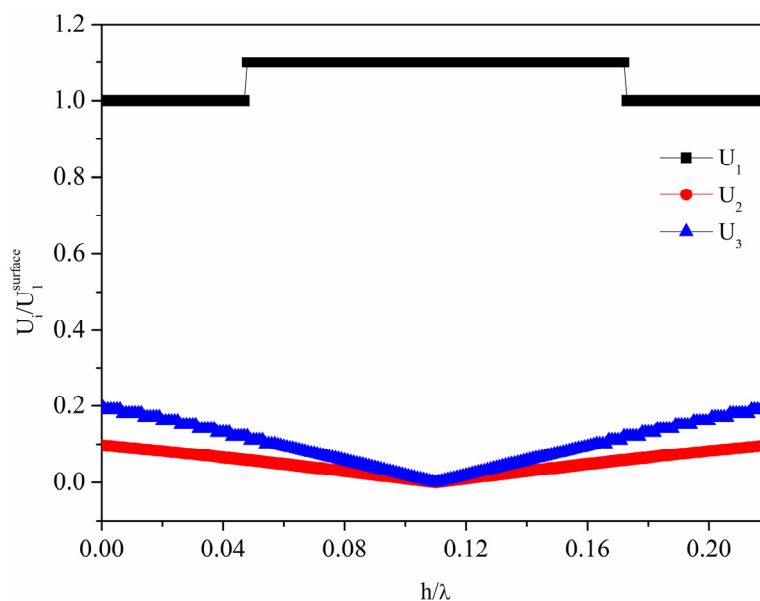
In the 60° to 90° range, the two coefficients A_1 and A_2 reach very small values, hence zero or very low TCD structures based on the AMs propagation can be fabricated.

The PFA is related to the incremental slope of the inverse velocity surface. The PFA of the AMs propagating along the x -axis of the unmetallized and metallized surface of the GaPO_4 plates was theoretically investigated in order to evaluate the effect of an electrical shorting layer on the plate surface on the PFA. In both the two cases the PFA is very small, in the 0 to 0.09 range, and it is poorly affected by the presence of a shorting layer on one plate surface.

2.4. The Quasi Longitudinal Modes

In the present paper, a mode is attributed to the QL-family if U_1 is not constant through the plate, and U_2 and U_3 are less than 20% of U_1 at any depth. As an example, Figure 13 shows the field profile of the QLM propagating along the $(0^\circ 0^\circ 0^\circ)$ x - GaPO_4 plate at $v = 4097$ m/s, being the plate thickness equal to $h/\lambda = 0.22$.

Figure 13. The field profile of the quasi longitudinal mode (QLM) propagating along the $(0^\circ 0^\circ 0^\circ)$ x - GaPO_4 plate with $h/\lambda = 0.22$ at $v = 4097$ m/s.

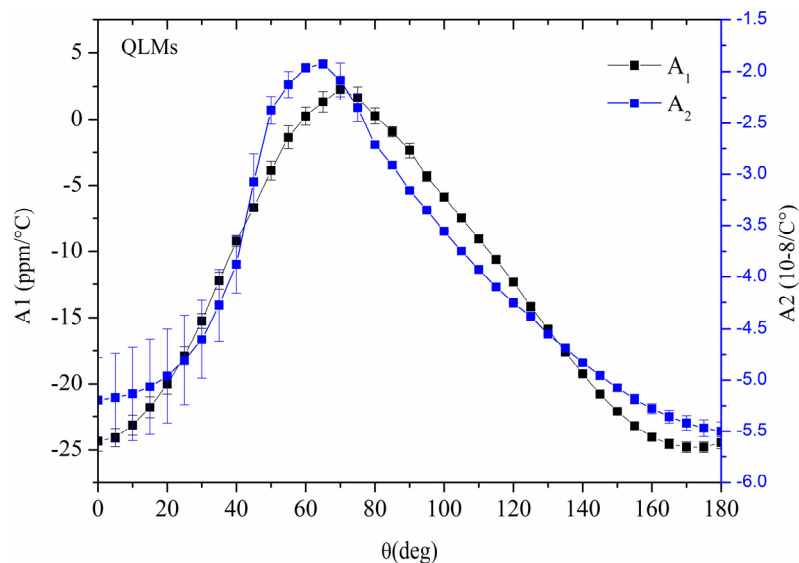


In Figure 14, the first and second order coefficients of the quadratic fit of the TCV vs. T °C of the QLMs are shown, being these coefficients calculated over the $h/\lambda_{\text{AMs}} - h/\lambda_{\text{QLM}}$ range, for each y rotation angle.

As compared with the AMs, the coefficients A_1 and A_2 of the QLMs are a little bit more temperature sensitive than those of the AMs.

As for the AMs, the PFA of the QLMs propagating along the x axis of y rotated GaPO_4 plates is very small, in the 0 to 0.09 deg range, and poorly affected by the presence of a metal shorting layer on the plate surface.

Figure 14. The first and second order coefficients of the quadratic fit of the TCV of the QLMs propagating along the ($0^\circ \theta 0^\circ$) GaPO₄ plate.



3. Conclusions

The phase velocity and the coupling coefficient of surface and flexural acoustic plate modes propagating along y -rotated x -propagation GaPO₄ piezoelectric substrates has been studied for several y -cut angles. The investigation of the acoustic field profile across the plate thickness revealed the presence of new viable modes, the linearly polarized Anisimkin Jr. and the quasi longitudinal plate modes, AMs and QLs, showing a phase velocity close to that of the longitudinal bulk acoustic wave propagating in the same direction. These modes are suitable for sensing applications in liquids (e.g., for the determination of density, viscosity, conductivity, permittivity, and detection of small mass changes). The TCD of these longitudinal modes was investigated in the -20 to 420 °C temperature range, in order to identify thermally stable or low TCD cuts. Thanks to the GaPO₄ intrinsic properties, such as its resistance to high temperature and its chemical inertness, electroacoustic devices based on the propagation of AMs in GaPO₄ are especially attractive for applications in harsh liquid environments. Moreover, such acoustic modes have not yet been fully exploited for sensing applications, thus their study introduces a new element in the landscape of the AW sensor field.

Author Contributions

Cinzia Caliendo conceived the research and conducted all the theoretical calculations, analyzed and processed the data, and wrote the manuscript. She is the Primary Investigator. Fabio Lo Castro assisted the data analysis for graphical outputs.

Conflicts of Interest

The authors declare no conflict of interest.

References

1. Ballantine, D.S.; White, R.M.; Martin, S.J.; Ricco, A.J.; Zellers, E.T.; Fye, G.C.; Wohltjen, H. *Acoustic Wave Sensors: Theory, Design, & Physico-Chemical Applications*; Levy, M., Stern, R., Eds.; Academic Press: Waltham Chestnut Hill, MA, USA, 1997.
2. Anisimkin, I.V. New type of an acoustic plate mode: Quasi-longitudinal normal wave. *Ultrasonics* **2004**, *42*, 1095–1099.
3. Gulyaev, Y.V. Propagation of the Anisimkin Jr.' plate modes in LiNbO₃ and Te single crystals. In Proceedings of the IEEE International Ultrasonics Symposium (IUS), Beijing, China, 2–5 November 2008.
4. Anisimkin, V. General Properties of the Anisimkin Jr. Plate Modes. *IEEE Trans. Ultrason. Ferroelectr. Freq. Control* **2010**, *57*, 2028–2034.
5. Anisimkin, V.I.; Pyataikin, I.I.; Voronova, N.V. Propagation of the Anisimkin Jr.' and Quasi-Longitudinal Acoustic Plate Modes in Low-Symmetry Crystals of Arbitrary Orientation. *IEEE Trans. Ultrason. Ferroelectr. Freq. Control* **2012**, *59*, 806–810.
6. Anisimkin, I.V.; Anisimkin, V.I. Attenuation of Acoustic Normal Modes in Piezoelectric Plates Loaded by Viscous Liquids. *IEEE Trans. Ultrason. Ferroelectr. Freq. Control* **2006**, *53*, 1487–1492.
7. PIEZOCRYST: Advanced Sensoristics GmbH. Available online: <http://www.piezocryst.com> (accessed on 30 April 2014).
8. Adler, E.L.; Farnell, G.W.; Slaboszewicz, J.; Jen, C.K. Interactive PC software for SAW propagation in anisotropic multilayers. In Proceedings of the IEEE Ultrasonics Symposium, San Diego, CA, USA, 27–29 October 1982.
9. Wallnofer, W.; Krempl, P.W.; Asenbaum, A. Determination of the elastic anti photoelastic constants of quartz-type GaPO₄ by Brillouin scattering. *Phys. Rev. B* **1994**, *49*, 10075–10080.
10. Reiter, C.; Krempl, P.W.; Wallnofer, W.; Leuprechth, G. GaPO₄: A Critical Review of Material Data. In Proceedings of the 9th EFTF, Besancon, France, 8–10 March 1995.
11. Shana, Z.; Josse, F. Analysis of liquid-phase-based sensors utilizing SH surface waves on rotated Y-cut quartz. In Proceedings of the 1988 Ultrasonics Symposium, Chicago, IL, USA, 2–5 October 1988.
12. Gizeli, E.; Stevenson, A.C.; Goddard, N.J.; Lowe, C.R. Acoustic Love plate sensors: Comparison with other acoustic devices utilizing surface SH waves. *Sens. Actuators B* **1993**, *13–14*, 638–639.
13. Kondoh, J. A Liquid-Phase Sensor Using Shear Horizontal Surface Acoustic Wave Devices. *Electron. Commun. Jpn.* **2013**, *96*, 41–49.
14. Anisimkin, V.I. General Properties of the Anisimkin Jr.' Plate Modes. In Proceedings of the 2009 IEEE International Ultrasonics Symposium, Roma, Italy, 20–23 September 2009.
15. Gulyaev, Y.V. Properties of the Anisimkin Jr.' Modes in Quartz Plates. *IEEE Trans. Ultrason. Ferroelectr. Freq. Control* **2007**, *54*, 1382–1385.